New Phytologist

UBC18 mediates ERF1 degradation under light–dark cycles

Mei-Chun Cheng, Wen-Chieh Kuo, Yi-Ming Wang, Hsing-Yu Chen and Tsan-Piao Lin

Institute of Plant Biology, National Taiwan University, 1 Roosevelt Road, Section 4, Taipei 10617, Taiwan

Author for correspondence:
Tsan-Piao Lin
Tel: +886 2 33662537
Email: tpl@ntu.edu.tw

Received: *10 May 2016*
Accepted: *11 September 2016*

New Phytologist (2017) **213:** 1156–1167
doi: 10.1111/nph.14272

Key words: abiotic stress, degradation, E2, Ethylene Response Factor 1 (ERF1), proline, ubiquitination, UBIQUITIN-CONJUGATING ENZYME 18 (UBC18).

Summary

• *Ethylene Response Factor 1* (*ERF1*) plays a crucial role in biotic and abiotic stress responses. Previous studies have shown that *ERF1* regulates stress-responsive gene expression by binding to different *cis*-acting elements in response to various stress signals. ERF1 was also reported to be unstable in the dark, and it regulates hypocotyl elongation. Here, we elucidated the mechanism underlying degradation of ERF1.

• Yeast two-hybrid screening showed that UBIQUITIN-CONJUGATING ENZYME 18 (UBC18) interacted with ERF1. The interaction between ERF1 and UBC18 was verified using pull-down assays and coimmunoprecipitation analyses. We then compared the ERF1 protein abundance in the *UBC18* mutant and overexpression plants. Based on the results of protein degradation and *in vivo* ubiquitination assays, we proposed that UBC18 mediates ERF1 ubiquitination and degradation.

• ERF1 was more stable in *UBC18* mutants and less stable in *UBC18* overexpression lines compared with that in wild-type plants. ERF1 was degraded by the 26S proteasome system via regulation of UBC18 and promotes dark-repression of downstream genes and proline accumulation.

• UBC18 negatively regulated drought and salt stress responses by altering the abundance of ERF1 and the expression of genes downstream of ERF1.

Introduction

Environmental stresses cause significant crop losses on an annual basis. A better understanding of the function of AP2/ERFs and other regulators involved in plant stress responses will contribute to our understanding of the molecular mechanisms underlying plant responses to environmental changes, which may ultimately be used for improvement of agricultural productivity. *ERF1* (*AT3G23240*) has been identified as a downstream component of the ethylene (ET) signaling pathway. Constitutive overexpression of *ERF1* in *Arabidopsis* resulted in resistance to *Botrytis cinerea* and *Plectosphaerella cucumerina* (Berrocal-Lobo *et al.*, 2002). *ERF1* is rapidly induced by ET and/or jasmonate (JA), and its expression can be synergistically activated by both hormones (Lorenzo *et al.*, 2003). Moreover, overexpressing *ERF1* can rescue the defense response defects in *coronatine insensitive1* (*coi1*) and *ethylene insensitive2* (*ein2*) mutants. These results indicate that ERF1 is a downstream component of the intersection between the ET and JA signaling pathways and integrates both signals to regulate defense response genes (Lorenzo *et al.*, 2003). Overexpressing *ERF1* activates the transcription of downstream effector genes, such as *basic-chitinase* (*b-CHI*) and *PLANT DEFENSIN1.2* (*PDF1.2*), and promotes ET responses (Solano *et al.*, 1998).

Our previous study revealed a dynamic role of ERF1 in both abiotic and biotic stress responses. We found that *ERF1* expression was rapidly and transiently induced by high salinity and dehydration treatments in an ABA-inhibited manner, and *35S:ERF1* transgenic *Arabidopsis* plants were more tolerant to drought, salt, and even heat stress. Transcriptome analysis of *35S:ERF1* and *ERF1* RNA interference (RNAi) knockdown plants showed that many stress-related genes, such as the *COR/RD* genes and heat shock-inducible genes, were up-regulated in *35S:ERF1* and conversely down-regulated in *ERF1* RNAi plants (Cheng *et al.*, 2013). Using chromatin immunoprecipitation (ChIP) assays, we identified a unique mechanism whereby ERF1 bound preferentially to different *cis*-elements of downstream genes following various types of stress signals (Cheng *et al.*, 2013).

Among the ERF1 downstream genes, *Δ^1-PYRROLINE-5-CARBOXYLATESYNTHETASE1* (*P5CS1*) encodes an important enzyme for proline biosynthesis. Proline is a proteinogenic amino acid with exceptional conformational rigidity and has an important function as a protective compatible osmolyte. Proline accumulation in stressed plants has a protective function, which has been demonstrated in numerous studies using transgenic plants or mutants (Szabados & Savouré, 2010). In our previous study, we showed that ERF1 directly and specifically activates the expression of *P5CS1* under high-salinity conditions and that proline accumulation increased in *ERF1* overexpression lines and decreased in RNAi lines (Cheng *et al.*, 2013). Moreover, it was reported that *P5CS1* induction and proline accumulation were light-dependent and inhibited in dark-adapted plants, but the underlying mechanism is still unknown (Abrahám *et al.*, 2003). Recently, ERF1 was also reported to be unstable under dark conditions and stable under light in 4-d-old *Arabidopsis* seedlings

and therefore regulated ET-induced hypocotyl elongation under light–dark cycles (Zhong *et al.*, 2012). However, further studies are needed to determine whether E3 ligase complexes are involved in modulating ERF1 protein stability.

Ubiquitination is one of the most studied post-translational modifications that modulate protein activities and plays important roles in various aspects of plant growth and development, including embryogenesis, floral development and plant senescence (Smalle & Vierstra, 2004; Dreher & Callis, 2007; Vierstra, 2009; Wang & Deng, 2011; Park *et al.*, 2012). Ubiquitination of a substrate promotes a cascade of enzymatic reactions: activating ubiquitin by an E1 ubiquitin activation enzyme with the hydrolysis of ATP, transferring ubiquitin to the E2 ubiquitin-conjugating enzyme, and then transferring the ubiquitin loaded on E2 to a substrate with the help of an E3 ubiquitin ligase (Ciechanover & Schwartz, 1998). E3 ligases are the key enzymes that determine substrate specificities and are mainly classified into four groups, including really interesting new gene (RING)/U-box, homology to E6-AP C-terminus (HECT), SKP1-CULLIN-F-box (SCF), and anaphase promoting complex (APC) (Vierstra, 2003). The roles of several RING domain-containing E3 ligases and E2 ligases have been implicated in photomorphogenesis, plant hormone signaling and defense responses (Qin *et al.*, 2008; Bu *et al.*, 2009; Ryu *et al.*, 2010; Li *et al.*, 2011; Cheng *et al.*, 2012; Liu *et al.*, 2012; Mural *et al.*, 2013; Xu *et al.*, 2014).

Protein substrates can be modified with a single ubiquitin protein (monoubiquitination) or a chain of ubiquitins (polyubiquitination) (Ikeda & Dikic, 2008). Ubiquitin is a highly conserved protein consisting of 76 amino acid residues with seven lysines, in which any one of the lysine residues might provide sites for polymerization. Polyubiquitin chains can be divided into seven types, including K6, K11, K27, K29, K33, K48 or K63. A prevalent function of polyubiquitination is to commit proteins to degradation by the 26S proteasome using the K11 and K48 chains as signals (Kim *et al.*, 2013). Proteins subjected to monoubiquitylation or modified with K63-linked Ub polymers direct nonproteolytic outcomes (Smalle & Vierstra, 2004; Chen & Sun, 2009; Lim & Lim, 2011; Kim *et al.*, 2013).

Here, we reported that an E2 ligase, UBC18, regulates *Arabidopsis* abiotic stress response by promoting ERF1 ubiquitination. Overexpression of *UBC18* resulted in an increase in ERF1 ubiquitination, which led to a decrease in ERF1 protein abundance and thus a reduction in the plant stress response. Conversely, down-regulation of UBC18 resulted in decreased ERF1 ubiquitination, which led to enhanced ERF1 accumulation and a better stress response. Our study revealed a mechanism that modulates the stability of ERF1 under light–dark cycles and regulates stress response.

Materials and Methods

Plant material and growth conditions

Seeds of the *Arabidopsis thaliana* L. Heynh. wild-type (WT, Columbia-0), *ubc18-1*, and *ubc18-2* mutants used in this study were obtained from the Arabidopsis Biological Resource Center. Potential *UBC18* (At5g42990) mutants were identified from Salk T-DNA lines (Alonso *et al.*, 2003) using the SiGnAL database (http://www.signal.salk.edu/cgi-bin/tdnaexpress). Genomic DNA from segregating plants was screened with PCR using SALK LB primers and UBC18 gene-specific primers to map the T-DNA insertion sites. For analysis of the *ubc18-1* line, annealing at 59°C was performed with the LBb1.3 primer and the following forward and reverse primers: LP2, 5′-AAGGTCGATGTT GACGAATTG-3′; and RP2, 5′-TCTCAATGCATCTAAAT CCGG-3′. For analysis of the *ubc18-2* line, annealing at 60°C was performed with the LBb1.3 primer and the following forward and reverse primers: LP1, 5′-AGCCTATCGAGTTC TTGGACC-3′; and RP1, 5′-CTCTGTGCTTAAACCCAG TCG-3′. The resulting PCR fragments were sequenced and compared with the genomic sequence for each gene to map the T-DNA insertion. The *35S:ERF1-GFP-His* transgenic plants were generated as described by Cheng *et al.* (2013). For normal growth conditions, seeds were surface-sterilized and germinated on Murashige and Skoog (MS) medium (pH 5.6) containing 1% sucrose and 0.7% phytoagar. Seedlings were grown under a 16 : 8 h, light : dark photoperiod at 22°C at a light intensity of 100–150 μmol m^{-2} s^{-1}.

Western blot analysis

For total protein extraction, the seedlings were ground in liquid nitrogen and dissolved in lysis buffer containing 2% sodium dodecyl sulfate (SDS), 60 mM Tris-HCl, pH 8.5, 2.5% glycerol, 0.13 mM EDTA, and 1X complete protease inhibitors (Roche). The protein concentration was determined using Bradford assays. BSA was used as a standard to calculate the coefficient. Total protein (100 μg) of each sample was separated using 10% Bis-Tris SDS-polyacrylamide gel electrophoresis and transferred to polyvinylidene difluoride membranes. The membrane was blocked with 5% non-fat milk in 1X phosphate-buffered saline (PBS) solution with 0.2% Tween 20 (PBST), pH 7.2, at room temperature for 60 min and hybridized with primary antibody in 5% nonfat milk solution for 1–2 h. The membrane was washed three times with 1X PBST for 5 min followed by hybridization with a horseradish peroxidase-conjugated secondary antibody in 3% nonfat milk solution for 1 h. After three washes in 1X PBST for 5 min and a rinse with distilled water, chemiluminescent substrates for signal detection were applied. Monoclonal mouse antibody against green fluorescent protein (GFP) was purchased from Santa Cruz Biotechnology (Santa Cruz, CA, USA).

RNA isolation and quantitative reverse transcription polymerase chain reaction (RT-PCR)

Total RNA was isolated using REzol C&T (PROtech Technologies; http://www.bio-protech.com.tw/) followed by treatment with DNase I (Ambion) before quantitative RT-PCR to eliminate genomic DNA contamination. cDNA was synthesized from 3 μg total RNA using Moloney murine leukemia virus reverse transcriptase (Invitrogen) with oligo (dT) primers. Quantitative RT-PCR was performed using the KAPA SYBR Green Premix

ExTaq (KAPA Biosystems, Wilmington, MA, USA) on a Bio-Rad MyiQ Real-Time PCR system according to the manufacturer's instructions. Relative expression levels were normalized to that of an internal control, *UBQ10*, under different light–dark conditions. However, under salt stress conditions, we used *ACT2* as the internal control. The expression patterns of *UBQ10* and *ACT2* under different light–dark conditions and salt stress are shown in Supporting Information Fig. S1.

Quantification of the Pro contents

Four-week-old *Arabidopsis* plants under normal growth conditions were used for measurement of Pro contents. Pro assays were performed as described by Bates *et al.* (1973) using lyophilized samples of *c.* 100 mg of plant material extracted in 2 ml of 3% aqueous sulfosalicylic acid. A total of 500 µl of filtrate was reacted with 2 ml ninhydrin and 500 µl of glacial acetic acid in a test tube for 1 h at 100°C, and the reaction was terminated in an ice bath. The reaction mixture was extracted with 1 ml toluene and mixed vigorously with a test tube stirrer for 15–20 s. The chromophore-containing toluene was aspirated from the aqueous phase and warmed to room temperature, and the absorbance was read at 520 nm using toluene for a blank. The Pro concentration was determined from a standard curve and calculated on a FW basis as follows: ((µg Pro ml^{-1} × ml toluene)/115.5 µg $µmol^{-1}$)/((g sample)/5) = µmol Pro g^{-1} FW material.

Drought and salt stress tolerance tests

For the drought tolerance test, 3-wk-old plants that were initially grown in soil under a normal watering regime were then dehydrated for 10–12 d, and observations were made. When WT plants exhibited lethal effects of dehydration, watering was resumed and the plants were allowed to grow for a subsequent 5 d. For the salt tolerance test, 3-wk-old plants were watered for 12 d at 4 d intervals with increasing concentrations of NaCl of 100, 200 and 300 mM. Survival was scored by examining the inflorescence base to determine if it still remained green. A plant was counted as a surviving plant when the leaf tissue, which is already present at the start of the assay, remained green near the inflorescence base.

Yeast two-hybrid screening

An *Arabidopsis* complementary (c)DNA library was prepared using the pGADT7 vector (MatchMaker GAL4 two-hybrid system 3; Clontech, http://www.clontech.com/) with mRNA isolated from 3-wk-old plants incubated in the dark for 2.5 h. Yeast transformation was performed according to the supplier's instructions (Clontech).

Bimolecular fluorescence complementation assays

ERF1 and UBC18 full-length sequences were cloned into the cYFP and nYFP vectors, respectively (Grefen *et al.*, 2010). Transient expression in *Arabidopsis* protoplasts was analyzed following Jen Shen's laboratory protocol (Yoo *et al.*, 2007). Yellow fluorescent protein (YFP) fluorescence was assessed with a laser scanning confocal microscope (Leica TCS SP5, Taipei, Taiwan).

Fusion protein preparation

Recombinant glutathione S-transferase (GST) fusion proteins were prepared as described in the GE protocol handbook (www.gelifesciences.com/protein-purification). Fragments encoding ERF1 were PCR-amplified from drought-treated cDNA samples and ligated into pGEX-6p-1 (Amersham-Pharmacia Biotech, Little Chalfont, UK). The resulting plasmids were transformed into *Escherichia coli* BL21 (DE3) cells and then induced using 1 mM Isopropyl β-D-1-thiogalactopyranoside (IPTG) for expression. Recombinant fusion proteins were affinity-purified from bacterial lysates using glutathione-Sepharose (Amersham-Pharmacia) according to the manufacturer's procedures and were then stored at −30°C. Recombinant thioredoxin (TRX)-hemagglutinin (HA) fusion proteins were prepared as follows. Full-length UBC18 coding sequence fragments were ligated into pET-32a. Recombinant fusion proteins were affinity-purified from bacterial lysates using glutathione-Sepharose (Amersham-Pharmacia) according to the manufacturer's procedures and then stored at −30°C.

Agrobacterium infection in *Arabidopsis* seedlings

AGROBEST infection assays were conducted as described in Wu *et al.* (2014). The disarmed strain of *Agrobacterium tumefaciens* (C58C1) was freshly streaked out from a −80°C glycerol stock onto a LB agar plate for a 2 d incubation at 28°C. A fresh single colony from the plate was used to inoculate 5 ml of LB liquid medium containing appropriate antibiotics for shaking (220 rpm) at 28°C for 20–24 h. For preinduction of *A. tumefaciens vir* gene expression, *A. tumefaciens* cells were pelleted and resuspended at an OD_{600} of 0.2 in various liquid media, including LB, LB-MES (LB with 10 mM MES, pH 5.7) or AB-MES (17.2 mM K_2HPO_4, 8.3 mM NaH_2PO_4, 18.7 mM NH_4Cl, 2 mM KCl, 1.25 mM $MgSO_4$, 100 µM $CaCl_2$, 10 µM $FeSO_4$, 50 mM MES, 2% glucose (w/v), pH 5.5) with different concentrations of acetosyringone (AS; 0, 50 or 200 µM) without antibiotics and then shaken (220 rpm) at 28°C for 12–16 h. Before infection, *A. tumefaciens* cells were pelleted and resuspended in the desired cocultivation liquid media to an OD_{600} of 0.02. The growth medium of *Arabidopsis* seedlings was replaced with 1 ml *A. tumefaciens* cells freshly prepared as described earlier and incubated in the same growth room for 3 d.

Results

ERF1 was degraded in the dark via the 26S proteasome system

To determine the stability of ERF1 protein in the dark, we generated transgenic *Arabidopsis* plants harboring an ERF1-GFP construct driven by the 35S promoter. As shown in Fig. 1(a),

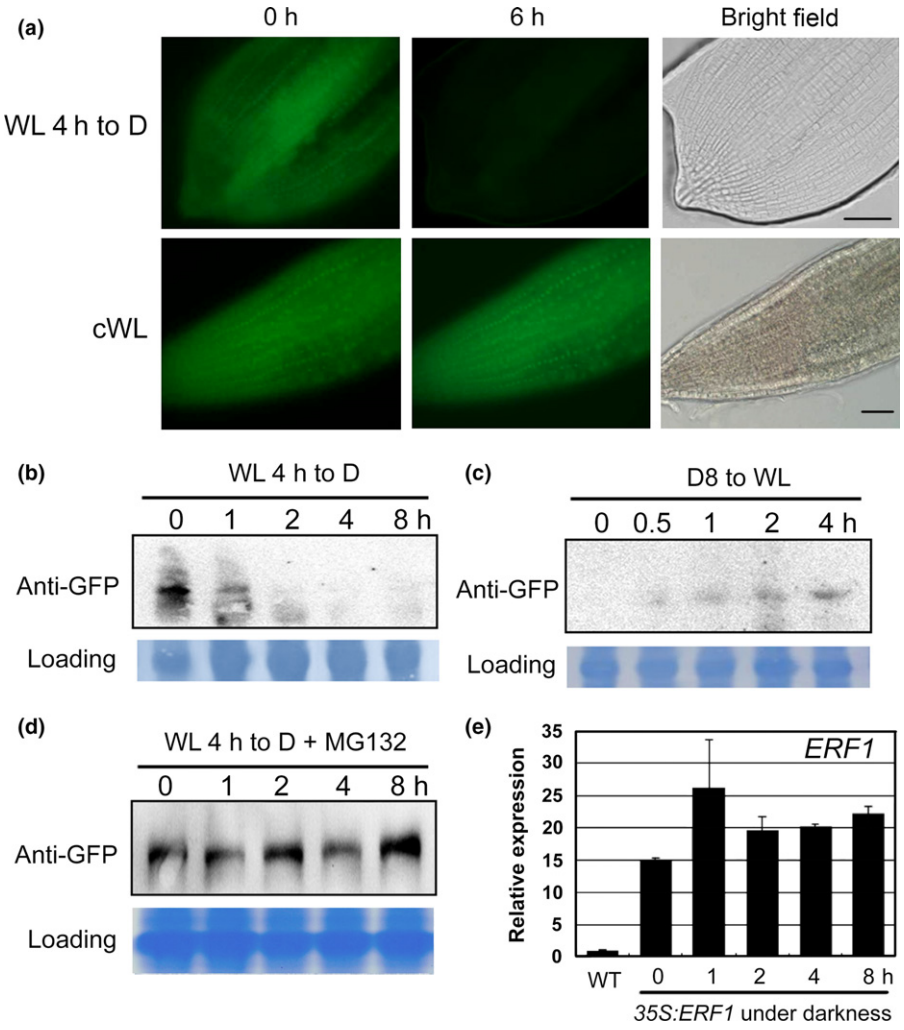

Fig. 1 ERF1 protein levels under dark incubation. (a) The upper panel shows that green fluorescent protein (GFP) signals in 4-d-old roots of *35S:ERF1-GFP* transgenic *Arabidopsis thaliana* plants become weaker after a 6 h dark incubation (WL 4h to D). The lower panel shows that GFP signals remain present under continuous light conditions (cWL). Bars, 10 μm. (b–d) Western blot analyses of ERF1 protein (by GFP antibody) in 15-d-old *35S:ERF1-GFP* plants. The plants grown on MS were first illuminated for 4 h and then incubated for up to 8 h in the dark (WL 4h to D, b, d) or first incubated in the dark for 8 h and then illuminated for up to 4 h (D8 to WL, c). (d) Western blot analysis of ERF1 protein in the *35S:ERF1-GFP* transgenic plants during dark incubation treated with MG132. Bars indicate SE. (e) *ERF1* expression in the *35S:ERF1-GFP* transgenic plants during dark incubation.

ERF1-GFP was microscopically observed in seedling roots following light exposure but disappeared after dark incubation for 6 h. As shown in western blot analyses (Fig. 1b,c), ERF1 protein was stabilized when the dark-grown plants were transferred to light exposure conditions. Conversely, ERF1 protein became unstable when light-exposed plants were returned to darkness. We then investigated whether the instability of ERF1-GFP protein in the dark was mediated by the 26S proteasome-dependent proteolysis system. As shown in Fig. 1(d), we found that the ERF1-GFP fusion protein in *35S:ERF1-GFP* plants remained abundant in dark conditions when treated with a proteasome inhibitor, carbobenzoxy-Leu-Leu-leucinal (MG132) (Fig. 1d). Although the *ERF1* transgene was overexpressed under all light conditions and did not appear to be affected after dark incubation (Fig. 1e), the corresponding protein was apparently unstable and may be degraded by the 26S proteasome.

To determine whether the expression of ERF1 downstream genes was influenced by the protein stability, we examined eight genes involved in different stress responses according to our previous study (Cheng *et al.*, 2013) in two independent *35S:ERF1* lines, including *b-CHI* and *PDF1.2* for biotic stress, *LATE EMBRYOGENESIS ABUNDANT PROTEIN4-5* (*LEA4-5*) and *At3g02480* for drought stress, *OSMOTIN34* (*OSM34*) and *P5CS1* for salt stress, and *HEAT SHOCK FACTORA3* (*HSFA3*) and *HEAT SHOCK PROTEIN101* (*HSP101*) for heat stress. As shown in Fig. 2(a), the expressions of most of these genes gradually decreased with dark incubation time. Our previous results also showed increased proline accumulation in *ERF1* overexpression lines and reduced accumulation in RNAi lines (Cheng *et al.*, 2013). As shown in Fig. 2(b,c), we also confirmed that proline accumulation was light-dependent even when *ERF1* was constitutively overexpressed. The results of the gene expression and proline content analyses are the average values of the two independent *35S:ERF1* transgenic plants (OE5 and OE6). These data indicated that ERF1 protein stability might play a major role in affecting proline accumulation in the dark by directly regulating *P5CS1* expression.

We further examined whether the dark repression of proline accumulation would affect salt stress tolerance in *35S:ERF1* plants. We first examined the salt stress induction of *P5CS1* under dark conditions. As shown in Fig. 3(a), the induction of *P5CS1* by salt stress treatment was inhibited after 8 h of dark incubation. In the salt stress tolerance tests, *35S:ERF1* plants grown in long-day conditions displayed tolerant phenotypes,

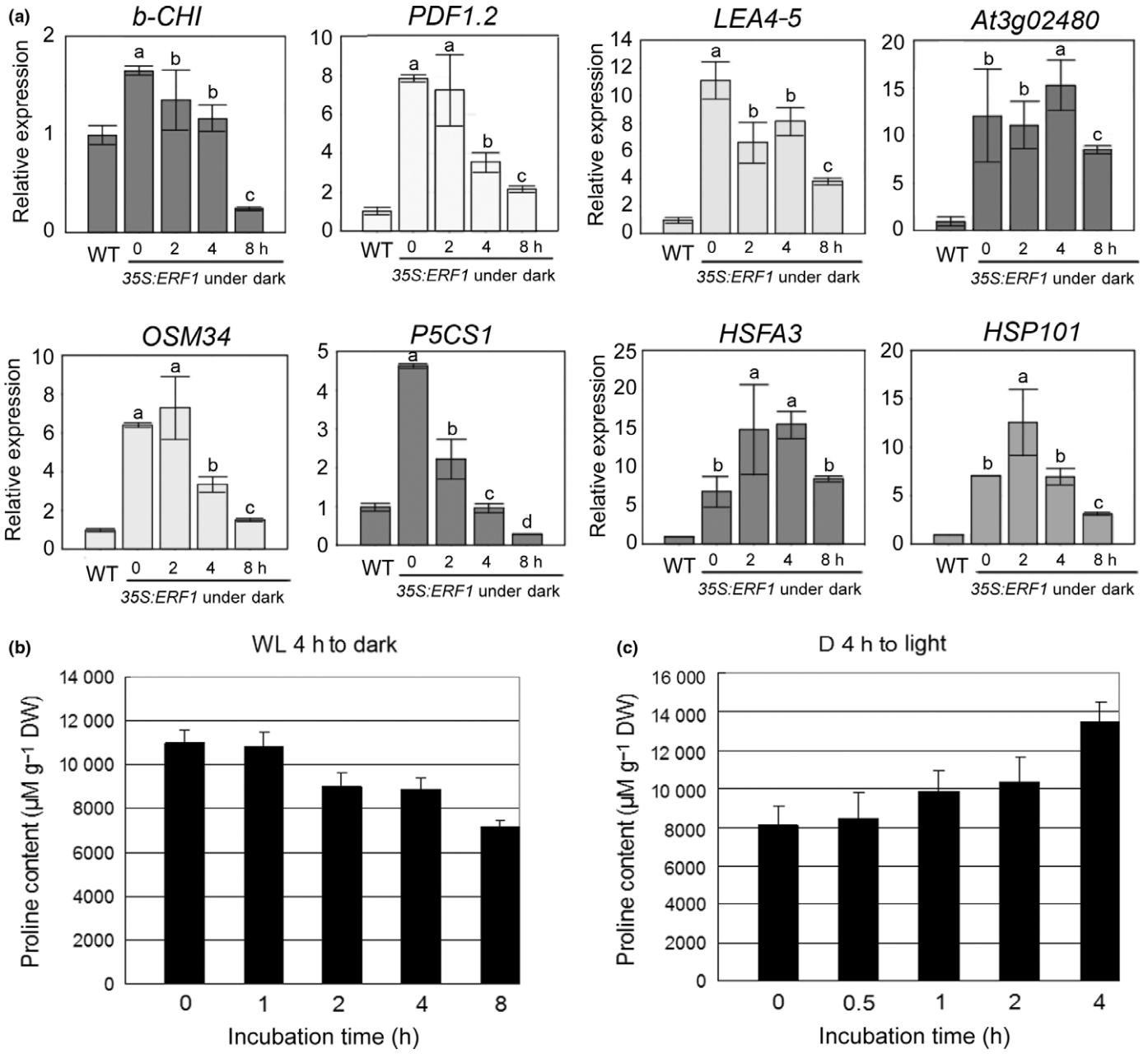

Fig. 2 The downstream gene expressions and proline accumulation are light-dependent in *35S:ERF1* transgenic *Arabidopsis thaliana* plants. (a) Expression of ERF1 downstream genes under dark conditions. Total RNA was prepared from 2-wk-old Col-0 (wild-type (WT), for normal light condition only) and *35S:ERF1* plants. The plants grown on Murashige and Skoog (MS) were first illuminated for 4 h and then incubated for up to 8 h in the dark. The relative mRNA levels of ERF1-upregulated genes were analyzed by quantitative reverse transcription polymerase chain reaction (RT-PCR) (the expression level of Col-0 was set to 1). *UBQ10* was used as an internal control. Data are shown as means ± SE of three replications. Different lower-case letters represent significant differences determined by Student's *t*-test at $P < 0.05$. (b, c) Two-week-old *35S:ERF1* plants grown on MS were first illuminated for 4 h and then incubated for up to 4 h in the dark (WL 4h to dark) (b) or first incubated in dark for 4 h and then illuminated for up to 4 h (D 4h to light) (c).

with a survival rate of *c.* 100% in contrast to 44% survival in WT plants, whereas the same OE line (OE5) grown in short-day conditions showed no significant difference in survival rate compared with that of the WT (Fig. 3b,c). Similar results were also observed in the other *35S:ERF1* line, OE6. This indicated that the salt stress-mediated induction of *P5CS1* was dark-inhibited, which might result in lower proline accumulation and lead to a more sensitive phenotype to salt stress.

ERF1 interacts with UBC18 *in vitro* and *in vivo*

To determine whether and how ERF1 is regulated at the protein level, we screened an *Arabidopsis* cDNA library by yeast two-hybrid (Y2H) assays for ERF1 interaction proteins. Full-length ERF1 was fused to the yeast GAL4 DNA-binding domain (BD) and used as a bait protein for screening against an *Arabidopsis* cDNA library (in the dark for 2.5 h) fused to the yeast GAL4

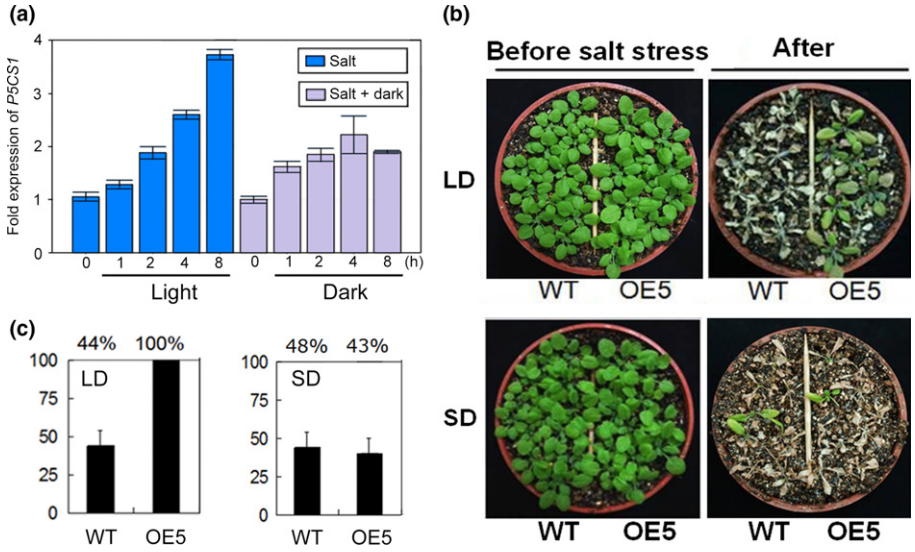

Fig. 3 Salt stress-induction of *P5CS1* in *ERF1*-overexpressing *Arabidopsis thaliana* plants under dark conditions and salt stress tolerance of *35S:ERF1* plants grown in long-day and short-day conditions. (a) Quantitative reverse transcription polymerase chain reaction analyses of *P5CS1*. Total RNA was prepared from 2-wk-old *35S:ERF1* plants treated with 150 mM NaCl in both light and dark conditions. Data are shown as means ± SE of three replications. (b) Survival of 3-wk-old plants grown in both long-day (16 : 8 h, light : dark, LD) and short-day (8 : 16 h, light : dark, SD) conditions were irrigated with different concentrations of NaCl solution (100 mM for 4 d, 200 mM for another 4 d, and 300 mM for the rest of the experiments). (c) Survival rate measurements in (b). WT, wild-type.

activation domain (AD). Approximately 1.2×10^6 yeast transformants were screened on a synthetic defined (SD) medium lacking Trp, Leu, and His (SD/-W-L-H) plus 30 mM 3-amino-1,2,4-triazole (3-AT). Fifty-one positive clones were obtained (Table S1). Among these candidates, we were predominantly interested in UBC18 (ubiquitin-conjugating enzyme E2 18), which putatively functions in targeting proteins for degradation.

To determine whether UBC18 actually interacts with ERF1 *in vitro*, we performed pull-down assays to test the interaction between the full-length UBC18 protein and ERF1. ERF1 was fused to the C-terminal of the GST tag in the pGEX-6p-1 vector, and UBC18 was fused to the Trx tag in the pET32a vector. As a result, the full-length Trx-UBC18 could be pulled down by GST-ERF1 (Fig. 4a). One-to-one Y2H was also carried out to further confirm their interaction. As a result, UBC18 was shown to have strong interactions with ERF1 (Fig. 4b). Furthermore, coimmunoprecipitation (CoIP) assays showed that HA-UBC18 coimmunoprecipitated with ERF1-GFP but not with GFP in tobacco (*Nicotiana tabacum*) leaves (Fig. S2), further confirming the interaction between UBC18 and ERF1 *in vivo*.

To further validate the interactions *in vivo*, we first determined the subcellular localization of UBC18 in protoplasts. Protoplasts were transformed with the *35S:UBC18-GFP* construct by polyethylene glycol-mediated transformation and assessed with fluorescence microscopy. As shown in Fig. S3, ERF1 was localized in the nucleus, whereas UBC18 localized in both the cytosol and nucleus. We then employed a bimolecular fluorescence complementation (BiFC) system to study their interaction in plant cells. The full-length UBC18 coding sequence (CDS) was fused to the N-terminal region of the YFP (YFP^N1-155, YN), and the ERF1 CDS was fused to the C-terminal region of YFP (YFP^C156-239, YC). The two constructs were cotransfected into *Arabidopsis* protoplasts. In parallel, the empty vectors in combination with each fusion construct were also transformed into the cells. After an overnight incubation, YFP signals were observed with fluorescence microscopy. Samples cotransfected by ERF1-YC and UBC18-YN yielded YFP fluorescence in the nucleus, whereas all of the samples cotransfected by the empty vector with either UBC18-YN or ERF1-YC failed to produce any YFP signal (Fig. 4d). These results indicate that UBC18 colocalizes and interacts with ERF1 in the plant cell nuclei.

UB18 regulates ERF1 protein abundance, and its ubiquitin conjugase activity is required for degradation of ERF1

We obtained two SALK T-DNA insertion lines from Ohio State University ABRC. As shown in Fig. 5(a,b), the T-DNA insertions in *UBC18* (SALK_084351 andSALK_107368) were confirmed by PCR using a T-DNA left border (LBb1.3) primer and gene-specific primers (RP2 for *ubc18-1* and RP1 for *ubc18-2*). Sequencing of the amplified fragment showed that the T-DNA insertions for *ubc18-1* and *ubc18-2* were at the border of the sixth exon and promoter, respectively (Fig. 5c). To determine whether expression of *UBC18* is altered in *ubc18-1* and *ubc18-2* homozygous mutant lines, we examined RNA levels using quantitative real-time PCR. We used RNA isolated from 2-wk-old plants grown under normal conditions, and *UBC18* gene-specific primers were used to determine the relative levels of *UBC18* (Fig. 5d). We found that *UBC18* expression was very low in *ubc18-1* mutants. Surprisingly, *ubc18-2* mutants had elevated *UBC18* gene expression (8.2-fold). *UBC18* full-length transcript was not detectable in *ubc18-1* mutants but was enhanced in *ubc18-2* mutants in our semiquantitative PCR results (Fig. S4).

To identify the role of ERF1 downstream of the UBC18 regulatory pathway, we assessed whether ERF1 was up-regulated in *UBC18* knockdown mutants and down-regulated in overexpression mutants. First, we compared the protein abundance of ERF1 between the WT and *ubc18-1* plants following dark incubation. Although the level of ERF1 in *ubc18-1* was significantly higher than that in WT before dark incubation, it still gradually declined in *ubc18-1* plants, similar to that in WT (Fig. 6a). Next, we compared the protein abundance of ERF1 between the WT and *ubc18-2* plants following dark incubation and found that there was almost no detectable ERF1 protein in *ubc18-2* compared with that of the WT (Fig. 6a). Furthermore, we also compared ERF1 levels in WT, *ubc18-1*, and *ubc18-2* plants that

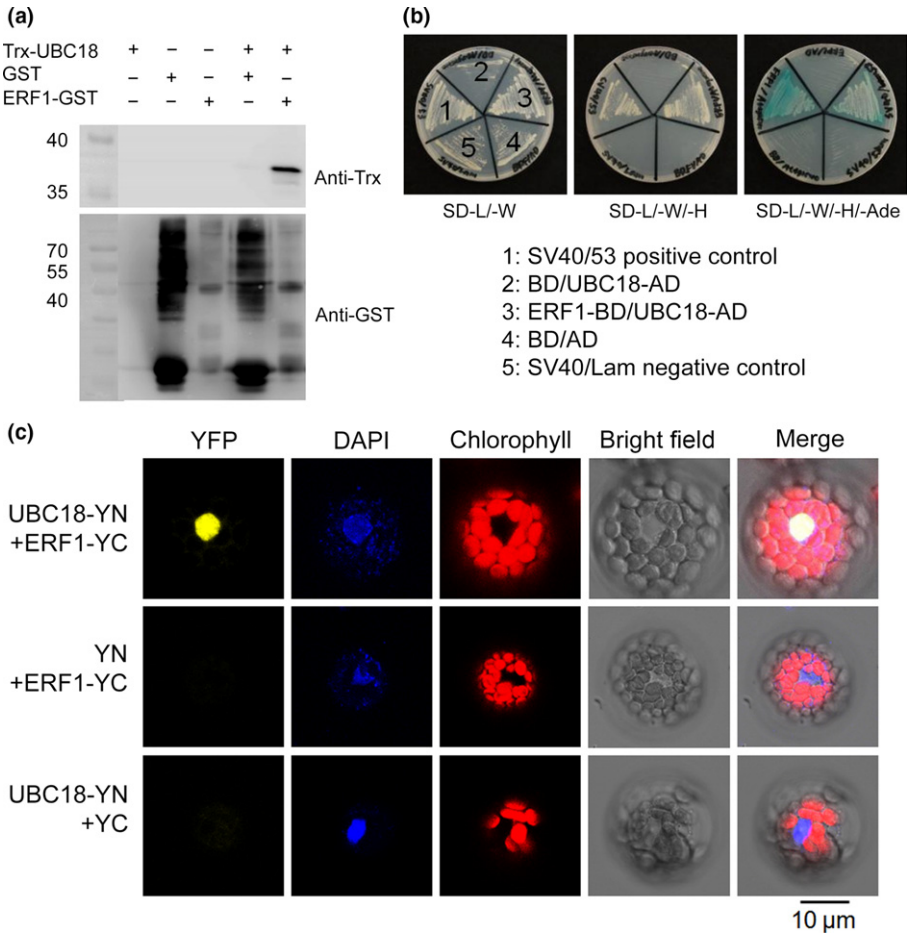

Fig. 4 ERF1 interacts with UBC18 *in vitro* and *in vivo*. (a) Pull-down assay showed that UBC18 can interact with ERF1. Purified Trx-UBC18 (lane 1), glutathione S-transferase (GST) (lane 2) and ERF1-GST (lane 3) were incubated with the lysis buffer as a negative control. Trx-UBC18 was incubated with GST alone (lane 4) or ERF1-GST (lane 5). The lower panel shows the same membrane probed with anti-GST antibodies. Experiments were repeated three times with the same results, and a representative experiment is shown. (b) Identification of UBC18 interactions with ERF1 via yeast two-hybrid analyses. Yeast cells transformed with UBC18-AD and ERF-BD growing on the selective medium and exhibiting β-galactosidase activity. (c) Interaction between ERF1 and UBC18 by bimolecular fluorescence complementation. Constructs of ERF1-YN, UBC18-YC and vice versa were cotransfected into *Arabidopsis* protoplasts. Yellow fluorescent protein (YFP) fluorescence, Chl, 4′,6′-diaminophenylindole (DAPI; for nuclear staining), and bright-field images are shown for each type of transformation combination.

recovered under light. As shown in Fig. 6(b), ERF1 levels gradually increased following light incubation in all these plants. However, ERF1 accumulated rapidly to a higher level in *ubc18-1* mutants, whereas it was recovered slowly in *ubc18-2* mutants compared with the WT plants (Fig. 6b). These results suggest that UBC18 is required for down-regulation of ERF1 under dark conditions.

To determine whether UBC18 serves as an intrinsic UBC enzyme involved in ERF1 degradation, we generated a mutant form of UBC18 where the conserved catalytic active residue Cys-99 was replaced with Ala. As shown in Fig. 7, when ERF1 and the WT form of UBC18 were coexpressed in tobacco (*Nicotiana tabacum*) leaves, the ERF1 level was reduced in a UBC18 dose-dependent manner (Fig. 7). However, the ERF1 level remained relatively constant when it was coexpressed with a mutant variant, $UBC18^{C99A}$ (Fig. 7). These results suggest that ERF1 was highly unstable when it was coexpressed with the catalytically active UBC18 and that UBC18 serves as a bonafide UBC enzyme for ERF1 degradation.

UBC18 mediates the ubiquitination of ERF1 proteins

To further assess whether UBC18 mediates the ubiquitination of ERF1, we detected the ubiquitinated proteins following immunoprecipitation *in vivo*. Using an *Agrobacterium*-mediated enhanced seedling transformation (AGROBEST) system generated by Wu *et al.* (2014), we transfected 4-d-old WT, *ubc18-1*, and *ubc18-2 Arabidopsis* lines with mock, *35S:GFP*, and *35S:ERF1-GFP* constructs. After a 3 d incubation, total proteins isolated from the WT, *ubc18-1*, and *ubc18-2* seedlings were subjected to immunoprecipitation analysis. Immunoprecipitation using an anti-GFP antibody successfully produced clear signals of GFP only and ERF1-GFP fusion proteins in seedlings transfected with *35S:GFP* and *35S:ERF1-GFP*, respectively, whereas anti-GFP antibodies yielded almost no signal in mock-treated seedlings after immunoprecipitation. When probed with an anti-ubiquitin antibody, the immunoprecipitated proteins showed a smear pattern at the higher molecular weights in the samples transfected with *35S:ERF1-GFP* but not in samples treated with mock and GFP-only controls, indicating the presence of polyubiquitinated or multi-monoubiquitinated ERF1 (Fig. 8). Whereas the protein level of ERF1-GFP was slightly increased in *ubc18-1* compared with the WT, the abundance of ubiquitinated ERF1 protein was moderately decreased. Moreover, we observed an increased abundance of ubiquitinated ERF1 in *ubc18-2* plants compared with the WT (Fig. 8). When we normalized the intensity of ubiquitination signals in WT, *ubc18-1*, and *ubc18-2* with the corresponding protein abundance of ERF1-GFP, a more prominent reduction and an increase in ubiquitinated ERF1 were detected in *ubc18-1* and *ubc18-2*, respectively. These results

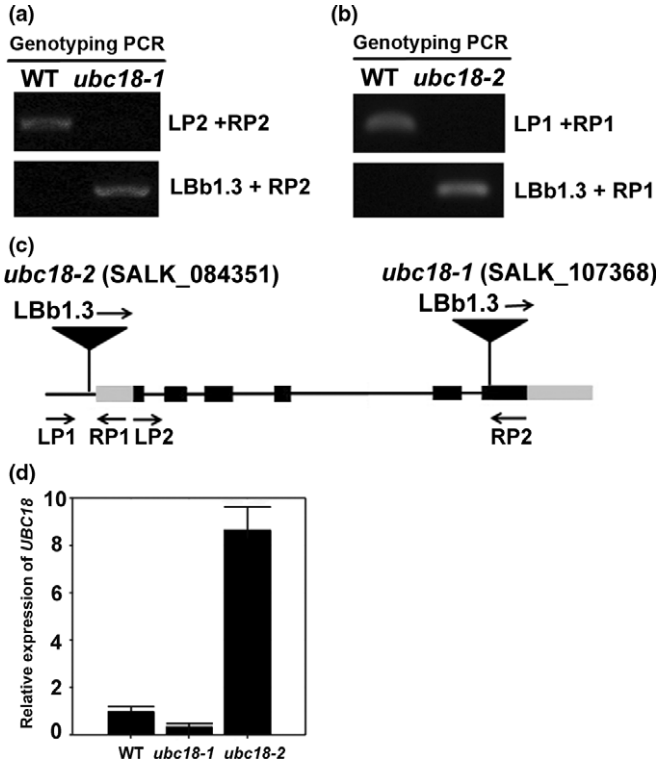

Fig. 5 Identification of the homozygous *UBC18* T-DNA-inserted *Arabidopsis thaliana* mutants. (a, b) Genotyping PCR analyses of the *ubc18-1* and *ubc18-2* mutants. Genotyping using PCR verified the homozygous *ubc18-1* and *ubc18-2* progeny. (c) Gene diagram of *UBC18* (At5g42990). Exons and introns are represented by boxes (black, coding region; gray, UTR) and lines, respectively. Black arrowheads depict T-DNA insertions. Primers used for genotyping PCR and reverse transcription polymerase chain reaction (RT-PCR) are shown with arrows. (d) Real-time quantitative RT-PCR analyses of the *ubc18-1* and *ubc18-2* mutants. RT-PCR indicated that *ubc18-1* is a knockdown mutant; *ubc18-2* is an overexpression mutant. *UBQ10* was used as an internal control. Bars indicate the SE.

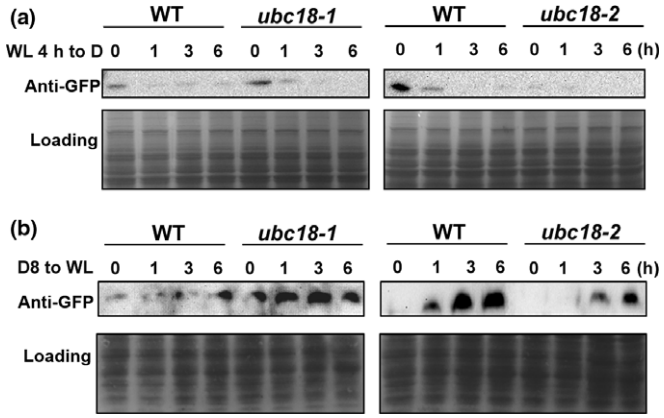

Fig. 6 UBC18 mediates ERF1 degradation under darkness. (a, b) Immunoblot analyses of ERF1 protein in 10-d-old wild-type (WT), *ubc18-1*, and *ubc18-2 Arabidopsis thaliana* plants on Murashige and Skoog (MS) medium treated with light irradiation (WL) for 4 h and then returned to darkness (a) or incubated in the dark for 8 h and then returned to light (b). Coomassie blue staining showed the protein amount loaded in each lane. Experiments were repeated three times with similar results, and a representative experiment is shown.

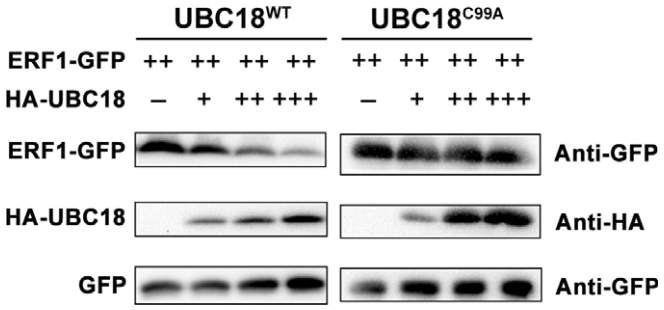

Fig. 7 UBC18 enzyme activity is required for degradation of ERF1. Immunoblot analyses of the expression of ERF1 when coexpressed with the functional $UBC18^{WT}$ or catalytically defective $UBC18^{C99A}$ in *Nicotiana benthamiana* leaves. Coinfiltration of the green fluorescent protein (GFP) was used as an internal control. Note that '+++' and '++' denote five- and 2.5-fold increases in the volume of infiltration relative to '+', respectively. –, not added. Experiments were repeated three times with similar results, and a representative experiment is shown.

support the hypothesis that UBC18 mediates the ubiquitination of ERF1 *in planta*.

UBC18 plays a negative regulatory role in drought and salt stress

To elucidate the role of UBC18 in abiotic stress, we used *ubc18-1* and *ubc18-2* mutants in drought and salt stress tests. In our assays aimed at detecting plant responses to prolonged periods of drought, *ubc18-1* plants revealed an improvement in their resistance to water deficit (Fig. 9a). After 18 d without watering, *ubc18-1* mutants remained nearly intact, without manifesting major macroscopic symptoms of drought-related stress compared with those of the WT plants. However, after 12 d without watering, *ubc18-2* mutants nearly collapsed and did not recover when watering was resumed, whereas WT plants remained vivid and green (Fig. 9b). After 18 d of drought stress, the survival rate for *ubc18-1* mutants was *c.* 70%, whereas only *c.* 33% of the WT plants survived (Fig. 9a). However, after 12 d of drought stress, the survival rate for *ubc18-2* mutants was *c.* 38%, whereas *c.* 60% of WT plants survived (Fig. 9b). Enhanced salt stress tolerance of *ubc18-1* mutants and decreased salt stress tolerance of *ubc18-2* plants were also observed (Fig. 9c,d). Plants were grown in normal conditions for *c.* 3 wk and then were watered with 100 mM saline for 4 d, 200 mM saline for another 4 d, and then 300 mM saline for the rest of the experiment. After salt stress treatment for 24 d, nearly all *ubc18-1* mutant plants survived, compared with only 30% of the WT plants (Fig. 9c). However, after salt stress treatment for 18 d, *c.* 35% of WT plants survived, compared with only *c.* 15% of the *ubc18-2* mutant plants (Fig. 9d).

To further show that UBC18 plays a negative role in stress response by regulating the protein abundance of ERF1, we analyzed the expression pattern of the same ERF1's downstream genes shown in Fig. 2(a) in WT, *ubc18-1*, and *ubc18-2* plants.

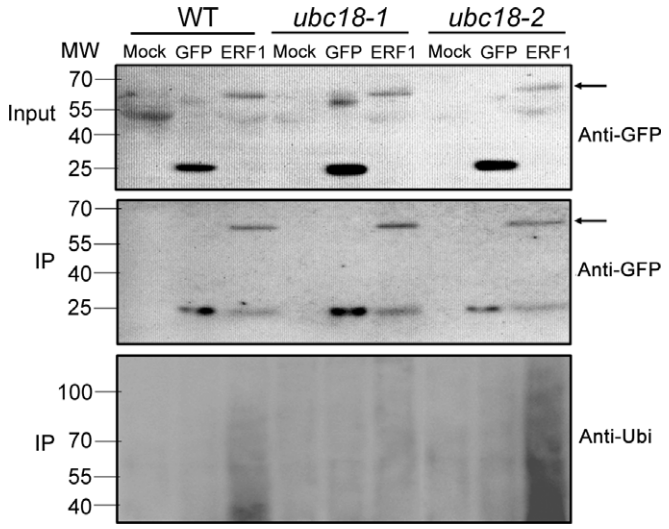

Fig. 8 UBC18 mediated the ubiquitination of ERF1. Immunoblot analysis by anti-GFP or anti-ubiquitin antibody following immunoprecipitation (IP) of total proteins. Total proteins were isolated from wild-type (WT), *ubc18-1*, and *ubc18-2 Arabidopsis thaliana* seedlings transfected with mock, green fluorescent protein (GFP) only, and ERF1-GFP using the AGROBEST system. Arrows indicate the ERF1-GFP fusion protein. MW, molecular weight.

Both under normal conditions (0 h) and salt stress treatment, the expressions of *OSM34* and *P5CS1* were higher in *ubc18-1* mutants but lower in *ubc18-2* mutants than those in WT plants (Fig. 9e). *PDF1.2* and *HSFA3* also showed higher expression in *ubc18-1* mutants but decreased expression in *ubc18-2* mutants (Fig. S5). The expression patterns of the genes, including *b-CHI*, *LEA4-5*, *At3g02480* and *HSP101*, were not altered in both *ubc18-1* and *ubc18-2* mutants compared with those in WT plants under salt stress conditions (Fig. S5). This is probably because ERF1 does not activate these genes under salt stress conditions (Cheng *et al.*, 2013). The reason why they were still induced by salt stress may be that there are other transcription factors regulating their expressions. By measuring the proline contents in WT, *ubc18-1* and *ubc18-2* mutant plants, we also found that *ubc18-1* mutants had higher proline accumulation, whereas *ubc18-2* mutants had lower proline levels, compared with those of the WT under normal conditions. When treated with 150 mM NaCl, both the mutants and WT plants showed increased proline accumulation (Fig. 9f). These results indicated that UBC18 negatively regulates drought and salt stress responses by altering the abundance of ERF1 and the expression of ERF1's downstream genes.

Discussion

To fine-tune the response to biotic and abiotic stresses, plants have developed a series of adaptive mechanisms involving transcriptional regulation of stress-responsive genes. Among them, the expression of *ERF1* is induced by drought and salt stress, in part through the ET signaling pathway (Cheng *et al.*, 2013). Alternatively, following pathogen attack, ET and JA signaling mediate the binding of EIN3 to the promoter of *ERF1* to induce the transcription of *ERF1* (Solano *et al.*, 1998). In this study, we further identified a layer of ERF1 regulation at the post-translational level by UBC18.

ERF1's stability may contribute to the light–dark oscillation of proline biosynthesis and many stress-responsive genes

We found that ERF1 declined rapidly in the dark, and when the 26S proteasome system was blocked by MG132, ERF1 was maintained for 8 h under dark conditions (Fig. 1b,d). This is consistent with the observations by Zhong *et al.* (2012) that ERF1-MYC is unstable in 4-d-old etiolated seedlings constitutively overexpressing *ERF1-MYC* when light-exposed seedlings were returned to darkness. In *ERF1* overexpression transgenic plants, many stress-related downstream genes of ERF1 and the proline content were decreased following dark incubation (Fig. 2). Among these genes, the salt stress-induced proline biosynthesis gene, *P5CS1*, was also repressed in the dark (Fig. 3a). This is consistent with the report by Hayashi *et al.* (2000) indicating that proline, as well as proteins and mRNAs of the synthetic enzymes, clearly oscillated in the light : dark cycles. *P5CS1* is known to be strongly up-regulated by unknown ABA-independent factors, with only a partial effect of ABA (Sharma & Verslues, 2010). ERF1 may be the unknown factor that exhibited strong binding affinity to the DRE element in the promoter of *P5CS1* during salt stress in an ABA-independent manner (Cheng *et al.*, 2013). ERF1 was reported to be a hub of ET and JA signaling (Solano *et al.*, 1998; Müller & Munné-Bosch, 2015). The induction of *ERF1* by drought and salt stress was even slightly inhibited by ABA in the early hours of induction (Cheng *et al.*, 2013). Additionally, recent data from our laboratory showed that proline induction by salt stress was inhibited in the ET-insensitive mutant *etr1*. Therefore, ET and JA signaling may play an important role in the salt stress-induced proline accumulation.

Recent studies have demonstrated a correlation between the circadian clock and plant responses to drought, suggesting a close connection between the light and stress signaling pathways (Legnaioli *et al.*, 2009; Wilkins *et al.*, 2010). Decreased susceptibility to *B. cinerea* was observed after inoculation at dawn compared with that at night under constant light conditions, demonstrating the role of the plant clock in driving time-of-day susceptibility to *B. cinerea* (Ingle *et al.*, 2015). Additionally, *Arabidopsis* has been shown to synchronize JA-mediated defense with insect circadian behavior (Goodspeed *et al.*, 2012). As a major signaling component of the JA and ET pathways, ERF1's reduced stability may play an important role in the susceptibility of plants to biotic stress in the dark. However, the improved salt stress tolerance of *ERF1* overexpression lines in long-day conditions (Fig. 3, or the higher stress-responsive gene expression under light conditions) prompted us to propose a hypothesis: during daylight hours, ERF1 may be stabilized to cope with environmental stress, such as higher temperature and transpiration rate and pathogen and bacterial attacks, which are increased during the day (Lozano-Durán & Zipfel, 2003, 2015). At night, ERF1 may be degraded to reduce energy consumption.

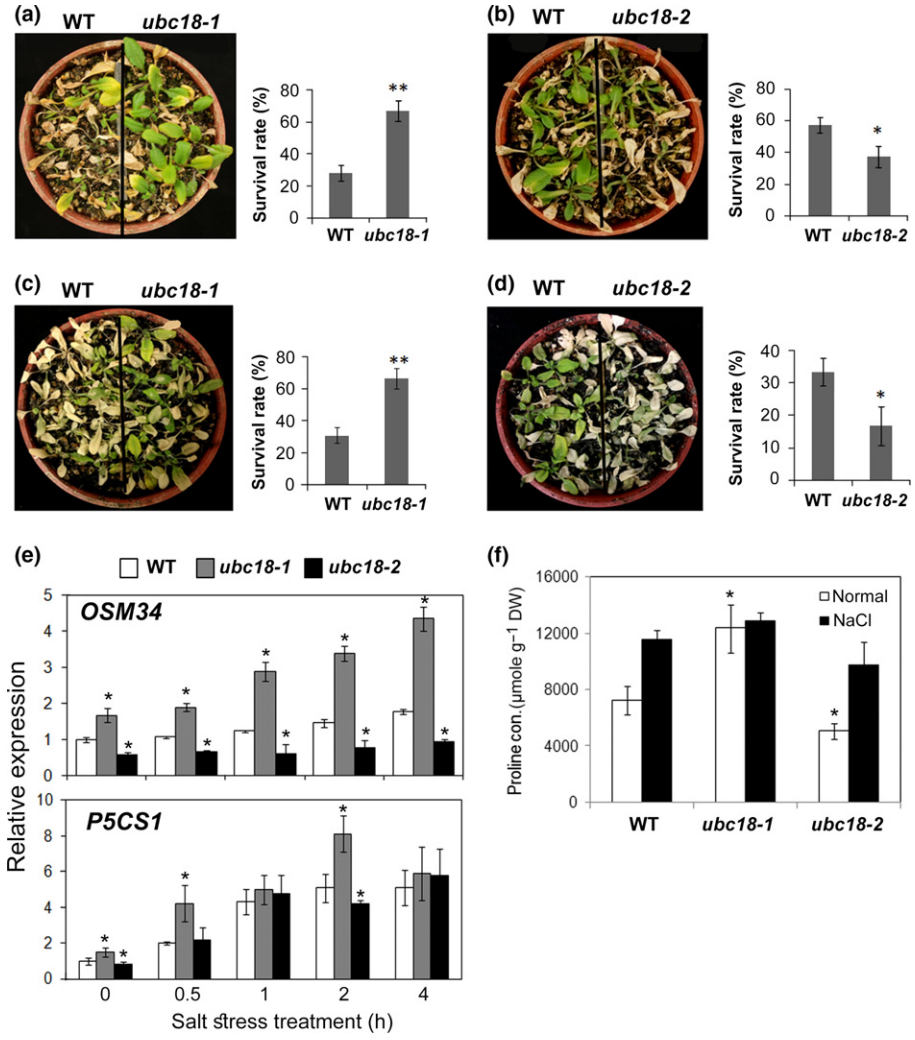

Fig. 9 Phenotypic analyses of *ubc18-1* knockdown and *ubc18-2* overexpression *Arabidopsis thaliana* mutants in response to drought and salt stress. (a, b) Drought-tolerant phenotypes of *ubc18-1* and drought-sensitive phenotypes of *ubc18-2* compared with that of the wild-type (WT). The results are averages of three replicates. Survival rates of WT, *ubc18-1* and *ubc18-2* plants under drought stress are shown on the side. (c, d) Salt-tolerant phenotypes of *ubc18-1* and salt-sensitive phenotypes of *ubc18-2* compared with that of the WT. The results are averages of three replicates. Survival rates of WT, *ubc18-1* and *ubc18-2* plants under salt stress are shown on the side. (e) Expression patterns of *OSM34* and *P5CS1* in WT, *ubc18-1* and *ubc18-2* plants under salt stress. (f) Proline contents in WT, *ubc18-1* and *ubc18-2* plants under salt stress. Error bars indicate ± SE (Student's *t*-test; *, $P < 0.05$; **, $P < 0.01$).

Although several post-translational mechanisms are involved in regulating transcription factor activities in response to light, such as phosphorylation, dimer formation, and ubiquitination (Jiao *et al.*, 2007), few were reported to be involved in abiotic stress response. SALT TOLERANCE HOMOLOG2 (STH2), also known as B-box transcription factor 24 (BBX24), confers salt stress tolerance to *Arabidopsis* and can interact with both HY5 and COP1 (Datta *et al.*, 2007). COP1 is known to negatively regulate HY5 under dark conditions by mediating its ubiquitination (Saijo *et al.*, 2003). Similar to ERF1, BBX24 is also regulated by light and participates in the abiotic stress response. Our studies identified an unexpected mode of light and ET-JA signal integration that results in improved stress tolerance.

UBC18 modulates ERF1 stability at the post-translational level

Using Y2H screening, we identified UBC18 as an interacting protein of ERF1. Our BiFC and CoIP results also suggested that there is a direct interaction between ERF1 and UBC18, and this interaction occurs in the nucleus (Fig. 4d). Notably, we showed that the degradation of ERF1 under dark conditions is slightly diminished in *UBC18* knockdown mutants but promoted in *UBC18* overexpression mutants (Fig. 6a,b), indicating that UBC18 mediates the post-translational down-regulation of ERF1. In our drought and salt stress tests, *ubc18-1* mutants showed better stress tolerance due to the higher ERF1 protein abundance, whereas *ubc18-2* exhibited a lower survival rate compared with that of the WT due to the reduced ERF1 protein (Fig. 9). These results indicate that UBC18 negatively regulates the abiotic stress response by modulating ERF1 stability. Based on our previous results, there was almost no expression of *ERF1* under normal conditions. *ERF1* was highly induced by abiotic stress but was not altered by the light : dark cycle (Cheng *et al.*, 2013; Fig. S6). However, *UBC18* is ubiquitously expressed, but its expression was not altered under both salt stress and the light : dark cycle (Fig. S6). As a result, ERF1 could only be regulated by UBC18 at the post-translational level under stress conditions. Our results also showed that ERF1 is unstable under dark conditions (Fig. 1), suggesting that ERF1 may be stabilized under light conditions by an unknown mechanism or that UBC18 specifically recognizes ERF1 under dark conditions.

The ubiquitination cascade is believed to involve the interaction of a specific E3 ligase (Ciechanover & Schwartz, 1998). However, recent studies have shown that many E2 proteins also interact with the substrates and regulate their stability. For example, huntingtin interacts with human ubiquitin-conjugating enzyme (hE2-25K) and is ubiquitinated (Kalchman *et al.*, 1996); NtUBC2 interacts with NtERF3 and promotes its degradation (Koyama *et al.*, 2013); and PHO2 (UBC24/PHOSPHATE 2) interacts with PHO1 and mediates PHO1 degradation to maintain Pi homeostasis (Liu *et al.*, 2012). Additionally, in 2005, Kraft *et al.* demonstrated that *Arabidopsis* UBC22, UBC19-20, and UBC1-6 had variable levels of E3-independent activity using an *in vitro* ubiquitination assay. Whether UBC18 functions as an E3-independent E2 or a chimeric E2-E3 enzyme for ERF1 ubiquitination remains to be confirmed by *in vitro* ubiquitination assays, but the results from the *in vivo* ubiquitination assays showed that UBC18 meditates the ubiquitination of ERF1 (Fig. 8).

In the protein abundance assay in Fig. 6, although there was more ERF1 in *ubc18-1* compared with the WT before dark incubation, ERF1 was still degraded after 3 h of dark incubation. This is probably because there is leaky expression of *UBC18* or leaky function of the truncated UBC18 without the protein part encoded by the sixth exon in *ubc18-1*. Whether the full-size CDS is needed to support full function of UBC18 and whether there are possible feedback effects of UBC18 on its own transcript abundance still require further investigation. There may also be other E2 or E3 enzymes mediating ERF1's degradation. PHOSPHATE TRANSPORTER1 (PHT1) was shown to be ubiquitinated and regulated by PHO2 (E2) in the endomembrane system (Huang *et al.*, 2013), whereas in the plasma membrane, it is also regulated by NITROGEN LIMITATION ADAPTATION (NLA), which is an E3 (Lin *et al.*, 2013). These findings suggest that a specific substrate may be targeted by different E2 or E3 enzymes in different cell compartments. Cao *et al.* (2008) also reported that two E2 enzymes, UBC1 and UBC2, and two E3 proteins, HISTONE MONOUBIQUITINATION1 (HUB1) and HUB2, are involved in the ubiquitination of HISTONE H2B and thus regulate the expression of *FLOWERING LOCUS C* (*FLC*); therefore, the *ubc1 ubc2* double mutants and the *hub1* and *hub2* mutants showed loss of H2B and the early flowering phenotype. These findings suggest that there may be other E2s or E3s involved in ERF1's stability. In photomorphogenesis, CONSTITUTIVE PHOTOMORPHOGENIC1 (COP1) is an important E3 enzyme that negatively regulates many components involved in light signaling (Lau & Deng, 2012). Because ERF1 was involved in hypocotyl elongation, Zhong *et al.* (2012) also hypothesized that COP1/SPA complexes modulate ERF1 stability.

Acknowledgements

This work was supported by the Ministry of Science and Technology, Taiwan (grant no. 104–2311–B–002–033–MY2 to T-P.L.).

Author contributions

M-C.C. and T-P.L. planned and designed the research. M-C.C., W-C.K. and Y-M.W. performed experiments. M-C.C. and H-Y.C. analyzed the data. M-C.C. and T-P.L. wrote the manuscript.

References

Abrahám E, Rigó G, Székely G, Nagy R, Koncz C, Szabados L. 2003. Light-dependent induction of proline biosynthesis by abscisic acid and salt stress is inhibited by brassinosteroid in Arabidopsis. *Plant Molecular Biology* **51**: 363–372.

Alonso JM, Stepanova AN, Solano R, Wisman E, Ferrari S, Ausubel FM, Ecker JR. 2003. Five components of the ethylene-response pathway identified in a screen for weak ethylene-insensitive mutants in Arabidopsis. *Proceedings of the National Academy of Sciences, USA* **100**: 2992–2997.

Bates LS, Waldren RP, Teare ID. 1973. Rapid determination of free proline for water-stress studies. *Plant and Soil* **39**: 205–207.

Berrocal-Lobo M, Molina A, Solano R. 2002. Constitutive expression of *ETHYLENE-RESPONSE-FACTOR1* in *Arabidopsis* confers resistance to several necrotrophic fungi. *Plant Journal* **29**: 23–32.

Bu Q, Li H, Zhao Q, Jiang H, Zhai Q, Zhang J, Wu X, Sun J, Xie Q, Wang D *et al.* 2009. The Arabidopsis RING finger E3 ligase RHA2a is a novel positive regulator of abscisic acid signaling during seed germination and early seedling development. *Plant Physiology* **150**: 463–481.

Cao Y, Dai Y, Cui S, Ma L. 2008. Histone H2B monoubiquitination in the chromatin of FLOWERING LOCUS C regulates flowering time in Arabidopsis. *Plant Cell* **20**: 2586–2602.

Chen ZJ, Sun LJ. 2009. Nonproteolytic functions of ubiquitin in cell signaling. *Molecular Cell* **33**: 275–286.

Cheng MC, Hsieh EJ, Chen JH, Chen HY, Lin TP. 2012. Arabidopsis RGLG2, functioning as a RING E3 ligase, interacts with AtERF53 and negatively regulates the plant drought stress response. *Plant Physiology* **158**: 363–375.

Cheng MC, Liao PM, Kuo WW, Lin TP. 2013. The Arabidopsis ETHYLENE-RESPONSE-FACTOR1 regulates abiotic-stress-responsive gene expression by binding to different cis-acting elements in response to different stress signals. *Plant Physiology* **162**: 1566–1582.

Ciechanover A, Schwartz AL. 1998. The ubiquitin-proteasome pathway: the complexity and myriad functions of proteins death. *Proceedings of the National Academy of Sciences, USA* **95**: 2727–2730.

Datta S, Hettiarachchi C, Johansson H, Holm M. 2007. SALT TOLERANCE HOMOLOG2, a B-box protein in *Arabidopsis* that activates transcription and positively regulates light-mediated development. *Plant Cell* **19**: 3242–3255.

Dreher K, Callis J. 2007. Ubiquitin, hormones and biotic stress in plants. *Annals of Botany* **99**: 787–822.

Goodspeed D, Chehab EW, Min-Venditti A, Braam J, Covington MF. 2012. Arabidopsis synchronizes jasmonate-mediated defense with insect circadian behavior. *Proceedings of the National Academy of Sciences, USA* **109**: 4674–4677.

Grefen C, Donald N, Hashimoto K, Kudla J, Schumacher K, Blatt MR. 2010. A ubiquitin-10 promoter-based vector set for fluorescent protein tagging facilitates temporal stability and native protein distribution in transient and stable expression studies. *Plant Journal* **64**: 355–365.

Hayashi F, Ichino T, Osanai M, Wada K 2000. Oscillation and regulation of proline content by P5CS and ProDH gene expressions in the light/dark cycles in *Arabidopsis thaliana* L. *Plant and Cell Physiology* **41**: 1096–1101.

Huang TK, Han CL, Lin SI, Chen YJ, Tsai YC, Chen YR, Chen JW, Lin WY, Chen PM, Liu TY *et al.* 2013. Identification of downstream components of ubiquitin-conjugating enzyme PHOSPHATE2 by quantitative membrane proteomics in Arabidopsis roots. *Plant Cell* **25**: 4044–4060.

Ikeda F, Dikic I. 2008. Atypical ubiquitin chains: new molecular signals. 'Protein modifications: beyond the usual suspects' review series. *EMBO Reports* **9**: 536–542.

Ingle RA, Stoker C, Stone W, Adams N, Smith R, Grant M, Carre I, Roden LC, Denby KJ. 2015. Jasmonate signalling drives time-of-day differences in

susceptibility of Arabidopsis to the fungal pathogen *Botrytis cinerea*. *Plant Journal* **84**: 937–948.

Jiao Y, Lau OS, Deng XW. 2007. Light-regulated transcriptional networks in higher plants. *Nature Reviews Genetics* **8**: 217–230.

Kalchman MA, Graham RK, Xia G, Koide HB, Hodgson JG, Graham KC, Goldberg YP, Gietz RD, Pickart CM, Hayden MR. 1996. Huntingtin is ubiquitinated and interacts with a specific ubiquitin-conjugating enzyme. *Journal of Biological Chemistry* **271**: 19385–19394.

Kim DY, Scalf M, Smith LM, Vierstra RD. 2013. Advanced proteomic analyses yield a deep catalog of ubiquitylation targets in Arabidopsis. *Plant Cell* **25**: 1523–1540.

Koyama T, Nii H, Mitsuda N, Ohta M, Kitajima S, Ohme-Takagi M, Sato F. 2013. A regulatory cascade involving class II ETHYLENE RESPONSE FACTOR transcriptional repressors operates in the progression of leaf senescence. *Plant Physiology* **162**: 991–1005.

Kraft E, Stone SL, Ma L, Su N, Gao Y, Lau OS, Deng XW, Callis J. 2005. Genome analysis and functional characterization of the E2 and RING-type E3 ligase ubiquitination enzymes of Arabidopsis. *Plant Physiology* **139**: 1597–1611.

Lau OS, Deng XW. 2012. The photomorphogenic repressors COP1 and DET1: 20 years later. *Trends in Plant Science* **17**: 584–593.

Legnaioli T, Cuevas J, Mas P. 2009. TOC1 functions as a molecular switch connecting the circadian clock with plant responses to drought. *The EMBO Journal* **28**: 3745–3757.

Li H, Jiang H, Bu Q, Zhao Q, Sun J, Xie Q, Li C. 2011. The Arabidopsis RING finger E3 ligase RHA2b acts additively with RHA2a in regulating abscisic acid signaling and drought response. *Plant Physiology* **156**: 550–563.

Lim KL, Lim GG. 2011. K63-linked ubiquitination and neurodegeneration. *Neurobiology of Disease* **43**: 9–16.

Lin WY, Huang TK, Chiou TJ. 2013. NITROGEN LIMITATION ADAPTATION, a target of microRNA827, mediates degradation of plasma membrane–localized phosphate transporters to maintain phosphate homeostasis in Arabidopsis. *Plant Cell* **25**: 4061–4074.

Liu TY, Huang TK, Tseng CY, Lai YS, Lin SI, Lin WY, Chen JW, Chiou TJ. 2012. PHO2-dependent degradation of PHO1 modulates phosphate homeostasis in Arabidopsis. *Plant Cell* **24**: 2168–2183.

Lorenzo O, Piqueras R, Sanchez-Serrano JJ, Solano R. 2003. ETHYLENE RESPONSE FACTOR1 integrates signals from ethylene and jasmonate pathways in plant defense. *Plant Cell* **15**: 165–178.

Lozano-Durán R, Zipfel C. 2015. Trade-off between growth and immunity: role of brassinosteroids. *Trends in Plant Science* **20**, 12–19.

Müller M, Munné-Bosch S. 2015. ethylene response factors: a key regulatory hub in hormone and stress signaling. *Plant Physiology* **169**: 32–41.

Mural RV, Liu Y, Rosebrock TR, Brady JJ, Hamera S, Connor RA, Martin GB, Zeng L. 2013. The tomato Fni3 lysine63-specific ubiquitin-conjugating enzyme and suv ubiquitin E2 variant positively regulate plant immunity. *Plant Cell* **25**: 3615–3631.

Park CH, Chen S, Shirsekar G, Zhou B, Khang CH, Songkumarn P, Afzal AJ, Ning Y, Wang R, Bellizzi M *et al.* 2012. The *Magnaporthe oryzae* effector AvrPiz-t targets the RING E3 ubiquitin ligase APIP6 to suppress pathogen associated molecular pattern-triggered immunity in rice. *Plant Cell* **24**: 4748–4762.

Qin F, Sakuma Y, Tran LS, Maruyama K, Kidokoro S, Fujita Y, Fujita M, Umezawa T, Sawano Y, Miyazono K *et al.* 2008. Arabidopsis DREB2A-interacting proteins function as RING E3 ligases and negatively regulate plant drought stress-responsive gene expression. *Plant Cell* **20**: 1693–1707.

Ryu MY, Cho SK, Kim WT. 2010. The Arabidopsis C3H2C3-type RING E3 ubiquitin ligase AtA IRP1 is a positive regulator of an abscisic acid-dependent response to drought stress. *Plant Physiology* **154**: 1983–1997.

Saijo Y, Sullivan JA, Wang H, Yang J, Shen Y, Rubio V, Ma L, Hoecker U, Deng XW. 2003. The COP1-SPA1 interaction defines a critical step in phytochrome A-mediated regulation of HY5 activity. *Genes & Development* **17**: 2642–2647.

Sharma S, Verslues PE. 2010. Mechanisms independent of abscisic acid (ABA) or proline feedback have a predominant role in transcriptional regulation of prolinemetabolism during low water potential and stress recovery. *Plant, Cell & Environment* **33**: 1838–1851.

Smalle J, Vierstra RD. 2004. The ubiquitin 26S proteasome proteolytic pathway. *Annual Review of Plant Biology* **55**: 555–590.

Solano R, Stepanovsa A, Qimin C, Ecker JR. 1998. Nuclear events in ethylene signaling: a transcriptional cascade mediated by ETHYLENE-INSENSITIVE3 and ETHYLENE-RESPONSE-FACTOR1. *Genes & Development* **12**: 3703–3714.

Szabados L, Savouré A. 2010. Proline: a multifunctional amino acid. *Trends in Plant Science* **15**: 89–97.

Vierstra RD. 2003. The ubiquitin/26S proteasome pathway, the complex last chapter in the life of many plant proteins. *Trends in Plant Science* **8**: 135–142.

Vierstra RD. 2009. The ubiquitin-26S proteasome system at the nexus of plant biology. *Nature Reviews Molecular Cell Biology* **10**: 385–397.

Wang F, Deng XW. 2011. Plant ubiquitin-proteasome pathway and its role in gibberellin signaling. *Cell Research* **21**: 1286–1294.

Wilkins O, Bräutigam K, Campbell MM. 2010. Time of day shapes Arabidopsis drought transcriptomes. *Plant Journal* **63**: 715–727.

Wu HY, Liu KH, Wang YC, Wu JF, Chiu WL, Chen CY, Wu SH, Sheen J, Lai EM. 2014. AGROBEST: an efficient *Agrobacterium*-mediated transient expression method for versatile gene function analysis in Arabidopsis seedlings. *Plant Methods* **10**: 19.

Xu D, Lin F, Jiang Y, Huang X, Li J, Ling J, Hettiarachchi C, Tellgren-Roth C, Holm M, Deng XW. 2014. The RING finger E3 ubiquitin ligase COP1 SUPPRESSOR1 negatively regulates COP1 abundance in maintaining COP1 homeostasis in dark-grown Arabidopsis seedlings. *Plant Cell* **26**: 1981–1991.

Yoo SD, Cho YH, Sheen J. 2007. Arabidopsis mesophyll protoplasts: a versatile cell system for transient gene expression analysis. *Nature Protocols* **2**: 1565–1572.

Zhong S, Shi H, Xue C, Wang L, Xi Y, Li J, Quail PH, Deng XW, Guo H. 2012. A molecular framework of light-controlled phytohormone action in Arabidopsis. *Current Biology* **22**: 1530–1535.

Supporting Information

Additional Supporting Information may be found online in the Supporting Information tab for this article:

Fig. S1 Expression patterns of *ACT2* and *UBQ10* under different light : dark conditions and salt stress treatment.

Fig. S2 Coimmunoprecipitation analysis of ERF1 interaction with UBC18 using tobacco transfection.

Fig. S3 Subcellular localization of ERF1 and UBC18 protein in Arabidopsis protoplast.

Fig. S4 Expressions of *UBC18* in *ubc18-1* and *ubc18-2* mutants.

Fig. S5 Expression patterns of ERF1's downstream genes in *UBC18* mutants under salt stress treatment.

Fig. S6 Expression profiles of *ERF1* and *UBC18*.

Table S1 Positive clones from yeast two-hybrid screening

Please note: Wiley Blackwell are not responsible for the content or functionality of any Supporting Information supplied by the authors. Any queries (other than missing material) should be directed to the *New Phytologist* Central Office.